

## NEURODEGENERATION CAUSED BY TRIMETHYLTIN VIA INHIBITION OF TROPOMYOSIN-RECEPTOR-KINASE B AND PHOSPHOINOSITIDE 3-KINASE/PROTEIN KINASE B SIGNALING CASCADE

Tran Phi Hoang Yen\*, Nguyen Ngoc Khoi, Duong Phuoc An, Nguyen Thi Thu Van, Do Minh Quang

University of Ho Chi Minh City, Faculty of Medicine and Pharmacy.  
41 Dinh Tien Hoang street, District 1, Ho Chi Minh City, Vietnam.

**Submitted:** 10-12-2013  
**Revised:** 12-01-2014  
**Accepted:** 13-03-2014

\*Corresponding author  
Tran Phi Hoang Yen

Email :  
tranyen73@gmail.com

### ABSTRACT

Trimethyltin (TMT, 2.4mg/kg, i.p) can trigger neuronal damage by inhibiting Tropomyosin receptor kinase B (TrkB receptor) following by phosphoinositide 3-kinase (PI3K)/protein kinase B or Akt signaling cascade. We examined hippocampal changes in TrkA/B phosphorylation on Tyr490/Tyr516 of TMT-treated mice in a time-dependent manner. Phosphorylated PI3K (Tyr508), phosphorylated 3-phosphoinositide-dependent protein kinase 1 (PDK1, Ser241) and phosphorylated Akt (Ser473) were changed following by TMT injury (from 3 hours until 7 days after injury). Treatment with 7,8-dihydroxyflavone (7,8-DHF), a specific agonist of TrkB, significantly attenuated the TMT-caused inhibition of phospho-TrkB, thereby increased in expressions of phospho-PI3K, phospho-PDK1 and phospho-Akt in TMT-treated mice, simultaneously 7,8-DHF showed a neuroprotective effect in observation of nuclear chromatic clumping by cresyl violet- and terminal deoxynucleotidyltransferase-mediated dUTP-biotin nick end labeling- (TUNEL) staining in the hippocampal dentate gyrus (DG) of TMT-treated mice, as compared to saline-treated group. This finding suggests that inhibition of TrkB receptor followed by PI3K/Akt cascade may play a part in the molecular mechanism by which TMT caused neurodegeneration in mice.

**Key words:** trimethyltin, neurodegeneration, TrkB receptor, PI3K/Akt pathway, mice

### INTRODUCTION

Selective neurodegeneration caused by trimethyltin (TMT) was demonstrated in the dentate gyrus of hippocampus of mice (Noriko *et al.*, 2010; Ogita *et al.*, 2005; Yoneyama *et al.*, 2008.) Until now, the molecular mechanisms underlying neuronal damage by TMT intoxication have remained unclear. We have previously reported the effect of TMT on the PI3K/Akt signaling cascade in a study designed to investigate the function of the interleukin-6 (IL-6) gene against neurotoxicity caused by TMT in the IL-6 knock-out mice. It was demonstrated that phospho-Akt (at Thr308) was decreased in the hippocampus of mice after TMT exposure, followed by the increase in the phosphorylation of Bad and the subsequent expression of Bcl-xL and Bcl-2. It was known that TrkB, a high attraction brain-derived neurotropic factor receptor, drives

signals through the PI3K and Ras pathways. So, TrkB interferes in the numerous effects of these neurotropic factors, which plays a crucial role in survival and differentiated-functions neurons (Calella *et al.*, 2007; Minichiello *et al.*, 1999). This study was built to expand on our anterior study and to understand better the regulation of the PI3K/Akt signaling pathway after TMT treatment as a function of time, we here focused on changes in phospho-TrkB and its downstream PI3K/Akt cascade from 3h to 7days after the administration of TMT. In the 7,8-DHF study, the presence of 7,8-DHF was reported to enhance the expressions of phospho-TrkB, phospho-PI3K, phospho-PDK1 and phospho-Akt in the hippocampus along with a simultaneous neurodegeneration in the hippocampus, which was detected using cresyl violet and TUNEL-staining.

## MATERIAL AND METHODS

### Animals

All mice were handled in strict accordance following the National Institutes of Health (NIH) Guide for the Humane Care and Use of Laboratory Animals (NIH Publication No. 85-23, 1985; [www.dels.nas.edu/ila](http://www.dels.nas.edu/ila)). *Swiss Albino* mice were supplied by the Institute of Vaccines and Medical Biologicals at Nha Trang Town, Vietnam. The male mice, weighing 24–28g, were maintained on a 12-h light/dark cycle and were fed *ad libitum*. They were allowed to adapt to these conditions for 1 week before the experiment.

### Drug treatment

TMT (Sigma-Aldrich) in sterile saline was prepared prior to be used. For TMT experiments, the mice received a single intraperitoneal (IP) injection of TMT (2.4mg/kg) or saline. The mice were then sacrificed at 3h, 6h, 12h, 1day, 2day, 3day and 7day after TMT treatment for western blotting analysis to detect TrkB and PI3K/Akt signals. For TrkB agonist experiments, 7,8-DHF (Sigma-Aldrich, St Louis, MO) was prepared in phosphate-buffered saline containing 17% of dimethylsulfoxide. The mice received a single dose of 7,8-DHF (10mg/kg, IP) 30min before they were injected with TMT. The mice were then sacrificed at 2d after TMT treatment for western blotting analysis to detect the TrkB and PI3K/Akt signals and neurodegenerative analysis using cresyl violet- and TUNEL-staining.

### Cresyl violet-staining

Cresyl violet-staining was performed as described previously (Kim *et al.*, 2002) to visualize the neuronal cell death in the hippocampus caused by TMT. A total nuclear clumping was conducted in the dentate gyrus of hippocampus. Every sixth section (7–10s per each brain sample) was applied for staining. Evaluation was performed on an Olympus microscope: OD 16592, Model: CX21, Olympus optical Co., Ltd.

### TUNEL staining

TUNEL staining was performed as described previously (Hoang-Yen *et al.*, 2012) using the TdT-FragEL DNA Fragmentation

Detection kit (Cat QIA33; Calbiochem, USA). The sections were incubated with 20mg/mL proteinase K and then with 3% hydrogen peroxide to block endogenous peroxidase activity. After that, the sections were immersed in the terminal deoxynucleotidyl transferase (TdT) equilibration buffer, biotinylated deoxynucleotides, TdT enzyme, and streptavidin–peroxidase complex, respectively. Then the sections were stained with diaminobenzidine and counter-stained with methyl green provided in the kit. Microphotographs were acquired at 40× or 100× magnification using an Olympus microscope: OD 16592, Model: CX21, Olympus optical Co., Ltd.

### Western blotting

Western blotting was performed as described previously. Hippocampal tissues were separated and kept frozen in liquid nitrogen. The samples were homogenized in lysis buffer, containing 200mM of Tris–HCl (pH 6.8), 1% of SDS, 5mM of ethylene glycol-*bis*(2-aminoethyl ether)-*N,N,N',N'*-tetra-acetic acid, 5mM of EDTA, 10% of glycerol, 1× phosphatase inhibitor cocktail I (Sigma–Aldrich) and 1× protease inhibitor cocktail (Sigma–Aldrich). The lysate was then centrifuged at 12,000×*g* for 30min to separate the supernatant fraction which was subjected to Western blotting. Proteins (20–50µg/lane) were separated by 8 or 10% of sodium dodecyl sulfate-polyacrylamide gel electrophoresis and then transferred onto polyvinylidene difluoride membranes. After that, the membranes were pre-incubated with 5% of nonfat milk for 30min and incubated overnight at 4°C with primary antibodies against β-actin (8H10D10) mouse mAb (1:10000, Sigma-R1281), anti-TrkB (Ab-705) antibody (1:1000, Sigma-SAB4300702), anti-phospho Trk A/B (Tyr490/Tyr516) (1:500, Cellsignaling, C50F3), anti-PDK1 antibody (1:1000, HPA027376, Sigma), anti-phospho-PDK1 (Ser241) (1:500, SAB4504514, Sigma), anti-PI3-K p85 antibody (1:1000, Sigma-HPA001216), anti-phospho PI3-K p85a (Tyr508) (1:500, Sigma-S8563), anti-Akt antibody (1:1000, Sigma-HPA002891) and anti-phospho Akt (Ser473) (1:500, Sigma-P4112). Then the membranes were incubated with anti-rabbit IgG (1:1000, Sigma-PM0100) or anti-mouse IgG (1:1000,

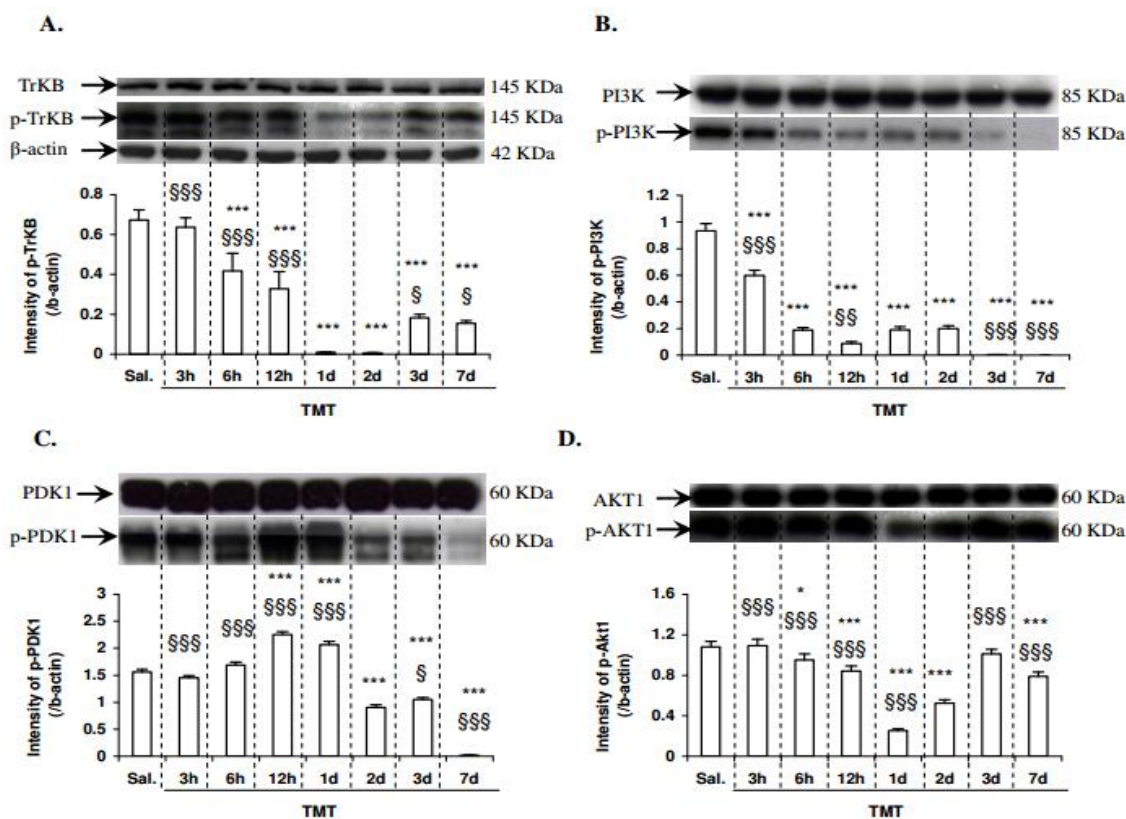


Figure 1. Time-dependent hippocampal changes in TrkB receptors, phospho-TrkA/B receptors (Figure 1A); in PI3K and phospho-PI3K (Figure 1B); in PDK1 and phospho-PDK1 (Figure 1C); in Akt and phospho-Akt (Figure 1D) of TMT-treated mice. Reductions in phospho-TrkA/B but not total TrkB were detected 3 h, 6 h, 12 h, 2 d, 3 d, and 7 d after TMT treatment. The reductions in phospho-PI3K, phospho-PDK1, and phospho-Akt were also detected time dependently. Each value is expressed as the mean±SEM of six mice. \* $P<0.05$ , and \*\*\* $P<0.001$  as compared to the saline-treated group; § $P<0.05$ , §§ $P<0.01$ , and §§§ $P<0.001$  as compared to the 2d after TMT-treated group (The data was analyzed using one-way ANOVA followed by Fisher's PLSD test).

Sigma-M6898) horseradish secondary peroxidase-linked for 2h. The membranes were then treated with chemiluminescence system (ECL Plus; GE Healthcare) for array visualization. The relative intensities of the bands were quantified by PhotoCapt MW (version 10.01 for Windows; Vilber Lourmat, Marne la Vallée, France).

### Statistical analysis

The data were displayed as means ± standard error and analyzed using a one-way ANOVA or a one-way ANOVA for repeated measures, followed by post hoc Fischer's PLSD

test. Values of  $P<0.05$  were considered as statistical significance.

### RESULTS AND DISCUSSION

It was proved that TMT was found in some areas of mouse's brain, such as the cerebellum, medulla-pons, hypothalamus, hippocampus, and striatum following the exposure of TMT (Cook *et al.*, 1984; Moser *et al.*, 2009) and it caused neuronal degeneration in the hippocampus of mice. Our study was performed to look for a reasonable molecular mechanism by which TMT causes neurodegeneration. Until now, the changes in

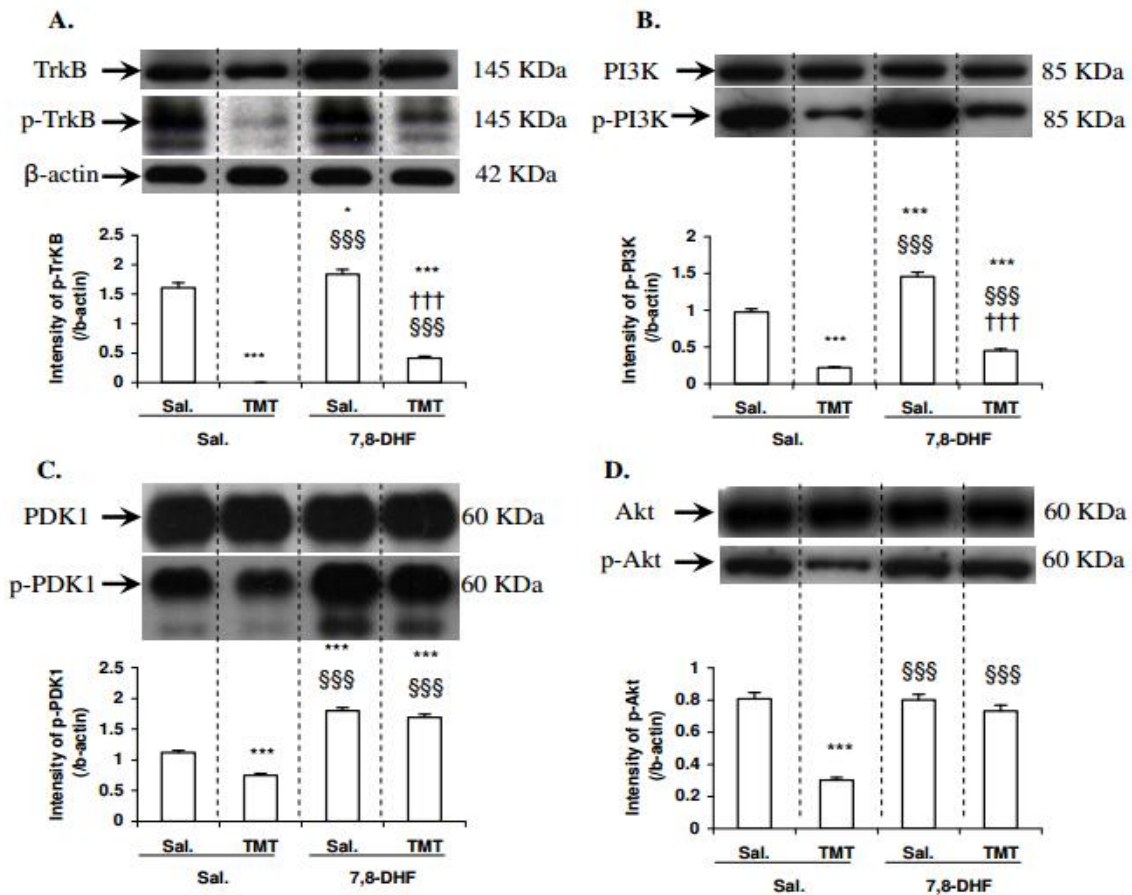


Figure 2. The effects of 7,8-DHF on TMT-induced change in TrkB receptors, phospho-TrkA/B receptors (Figure 2A); in PI3K and phospho-PI3K (Figure 2B); in PDK1 and phospho-PDK1 (Figure 2C); in Akt and phospho-Akt (Figure 2D). Each value is expressed as the mean±S.E.M of six mice. \* $P < 0.05$ , \*\*\* $P < 0.001$  as compared to the saline-treated group; \$\$\$ $P < 0.001$  as compared to the 2d after TMT-treated group; ††† $P < 0.001$  as compared to 7,8-DHF-treated group (The data was analyzed one-way ANOVA followed by Fisher's PLSD test).

TrkB in the hippocampal DG of TMT-exposed mice were not observed. One study on rats indicated that the decrease in TrkB mRNA was seen in the pyramidal cells of CA3 region 3 days after the exposure of TMT (Andersson *et al.*, 1997). Consistent with this finding, our data from current study showed that TMT inhibited activation of TrkB receptor, as using western blotting analysis. Although no changes of TrkB in the mouse hippocampal DG from 3h to 7d following a single dose of TMT were detected, dramatic decreases in p-TrkA/B receptor were detected from 6h to 7d post-TMT administration, with the largest decrease occurring at 2d (data are shown in figure 1A: the

expression of p-TrkA/B density of 3h post-TMT group/ $\beta$ -actin:  $0.637 \pm 0.047$ ,  $P = 0.62$ ; 6h post-TMT  $0.417 \pm 0.089$ ,  $P = 9 \times 10^{-4}$ ; 12h post-TMT  $0.328 \pm 0.086$ ,  $P = 2.09 \times 10^{-5}$ ; 1d post-TMT  $0.009 \pm 0.002$ ,  $P = 1.57 \times 10^{-11}$ ; 2d post-TMT  $0.006 \pm 0.020$ ,  $P = 1.39 \times 10^{-11}$ ; 3d post-TMT  $0.183 \pm 0.017$ ,  $P = 3.13 \times 10^{-8}$ ; 7d post-TMT  $0.155 \pm 0.013$ ,  $P = 8.84 \times 10^{-9}$ , compared with the control group). Interestingly, the expression of p-TrkA/B was almost disappeared at 2d post-TMT, correlated with neurodegenerative data which was assessed by cresyl violet- and TUNEL-staining. This suggests that TMT may directly or indirectly affect phosphorylation of TrkB, leading to subsequent changes in its

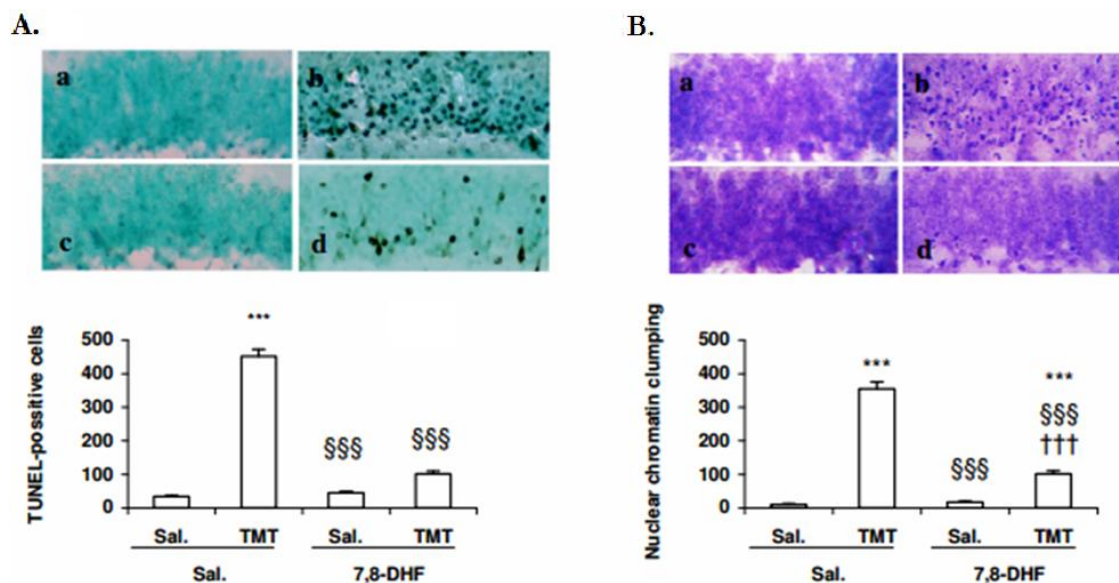


Figure 3. In the presence of 7,8-DHF, TMT-induced TUNEL-positive cells (Figure A - a, saline; b, TMT; c, 7,8-DHF 10 mg/kg; d, 7,8-DHF 10 mg/kg +TMT) and nuclear chromatin clumping counts assessed by cresyl violet staining (Figure B - a, saline; b, TMT; c, 7,8-DHF 10 mg/kg; d, 7,8-DHF 10 mg/kg +TMT) were observed. Each scale bar = 100µm. Each value is expressed as the mean±S.E.M of six mice. \* $P<0.05$ , \*\*\* $P<0.001$  as compared to the saline-treated group; SSS $P<0.001$  as compared to the 2d after TMT-treated group; ††† $P<0.001$  as compared to 7,8-DHF-treated group (The data was analyzed one-way ANOVA followed by Fisher's PLSD test).

downstream molecular signaling, inducing the neuronal toxicity. Moreover, to address whether TMT has a time-dependent impact on p-PI3K or not, western blot analysis for PI3K and constitutive activation of PI3K were performed. We found that p-PI3K was decreased in the hippocampus of TMT-treated mice, whereas the total PI3K changes were not detected. These changes were evident early after TMT treatment (data are shown in figure 1B: the expression of protein density of 3 h post-TMT group/ $\beta$ -actin:  $0.598\pm 0.039$ ,  $P=1.34\times 10^{-10}$ ; 6h post-TMT  $0.187\pm 0.019$ ,  $P=1.05\times 10^{-21}$ ; 12h post-TMT  $0.086\pm 0.014$ ,  $P=1.03\times 10^{-23}$ ; 1d post-TMT  $0.190\pm 0.023$ ,  $P=1.21\times 10^{-21}$ ; 2d post-TMT  $0.199\pm 0.022$ ,  $P=1.93\times 10^{-21}$ ; 3d post-TMT  $0.003\pm 0.001$ ,  $P=3.12\times 10^{-25}$ ; 7d post-TMT  $0.000\pm 0.000$ ,  $P=2.81\times 10^{-25}$ , compared with the saline group). Following the time-dependent decrease in p-PI3K in TMT-exposed mice, the changes of PDK1 and p-PDK1 were evaluated to address whether TMT neuro-toxicity had any impact on the PI3K/Akt cascade. In early term course

after TMT injury, no change of p-PDK1 was detected (data are shown in figure 1C:  $P=0.057$  and  $P=0.656$  for 3h and 6h-post TMT vs. saline, respectively). Significant increases in p-PDK1 were noted in 12 h and 1 d post-TMT injury (data are shown in figure 1C: the density of protein expressions of 12h post-TMT group/ $\beta$ -actin:  $2.251\pm 0.058$ ,  $P=1.04\times 10^{-6}$  and 1d post-TMT  $2.063\pm 0.062$ ,  $P=3.26\times 10^{-5}$ , compared with the saline group). Downregulation of p-PDK1 in the hippocampus was observed from 2d to 7d post-TMT administration (data are shown in Figure 1C: the expression of protein density of 2d post-TMT group/ $\beta$ -actin:  $0.900\pm 0.052$ ,  $P=4.85\times 10^{-11}$ ; 3d post-TMT  $1.048\pm 0.039$ ,  $P=9.3\times 10^{-10}$ , and 7d post-TMT  $0.017\pm 0.006$ ,  $P=1.13\times 10^{-19}$ , compared with the saline group). Akt phosphorylated was decreased in the hippocampus from 6h until 7d of TMT treatment (data are shown in figure 1D: the expressions of p-Akt density of 3h post-TMT group/ $\beta$ -actin:  $1.091\pm 0.053$ ,  $P=0.008$ ; 6h post-TMT  $0.952\pm 0.050$ ,  $P=0.783$ ; 12h

post-TMT  $0.842 \pm 0.041$ ,  $P=0.125$ ; 1d post-TMT  $0.252 \pm 0.017$ ,  $P=2.87 \times 10^{-14}$ ; 2d post-TMT  $0.524 \pm 0.035$ ,  $P=5.5 \times 10^{-9}$ ; 3d post-TMT  $1.010 \pm 0.050$ ,  $P=0.075$ ; 7d post-TMT  $0.787 \pm 0.040$ ,  $P=0.004$ , compared with the saline group). The survival and differentiated neurons were affected by Trk receptors through some signal transduction cascade, such as cell survival PI3K/Akt cascade (Huang *et al.*, 2003). Once phosphorylated, Trk receptors activated the survival and differentiated neurons, such as stimulating the P13 heterodimers, caused the phosphorylation of PDK-1 and Akt (Segal *et al.*, 2003). To investigate whether the neurodegeneration induced by TMT in mice model was due to inhibition of TrkB receptor or not, 7,8-DHF was administrated to assess the changes in p-TrkB, p-PI3K, p-PDK1 and p-Akt in mouse hippocampi at 2d after TMT treatment. Two days after TMT treatment, the changes in p-TrkB and others indexes were more pronounced, so this time point was chosen in 7,8-DHF study. Pretreatment with 7,8-DHF 30min before TMT attenuated inhibition of p-TrkB, p-PI3K, p-PDK1 and p-Akt expressions. Data are shown in figure 2A: the expression of p-TrkA/B density of 7,8-DHF + TMT group/ $\beta$ -actin:  $0.413 \pm 0.031$ ,  $P=1 \times 10^{-4}$ , compared with the TMT group. Data are shown in figure 2B: the expression of p-PI3K density of 7,8-DHF + TMT group/ $\beta$ -actin:  $0.452 \pm 0.022$ ,  $P=3 \times 10^{-4}$ , compared with the TMT group. 7,8-DHF was also showed a neuroprotective effect in TMT mouse model using Cresyl violet- (figure 2C) and TUNEL-staining (figure 2D). Two days after TMT administration, neurodegeneration and neuronal loss were obviously detected in the DG of mouse's hippocampi (Figure 3B-b). TUNEL-staining was applied for detecting the presence of fragmented DNA in hippocampal samples. The results revealed that very few TUNEL-positive were noted in the hippocampal DG of saline-treated mice, while the total of TUNEL-positive cells was significantly increased in TMT-treated mice ( $P < 0.001$ , as compared to the saline-treated group). Simultaneously, a very few of nuclear chromatin clumping was detected in the saline-treated mice, while this signal dramatically increased in the TMT-treated mice ( $P < 0.001$ , as

compared to the saline-treated group). 7,8-DHF-treated mice showed a significant attenuates neuronal toxication induced by TMT as showed by cresyl violet- and TUNEL-staining data (Figure 3).

## CONCLUSION

The main purpose of the present study is to elucidate the molecular mechanisms by which trimethyltin (TMT)-mediated neuronal degeneration occurs. Our research suggests that the inhibition of activated-TrkB receptor in mice caused by TMT intoxication is an important initial step toward neurodegenerative process. That was PI3K/Akt signaling pathway, including the decrease in the expressions of p-PI3K, p-PDK1 and p-Akt in the hippocampal DG of mice. Although we could not demonstrate that TMT causes neurodegeneration via binding to TrkB receptor then inhibits this receptor, at least we could say that TMT may produce neurodegenerative effect via inhibiting TrkB receptor and it's a downstream, PI3K/Akt cell survival signaling pathway.

## ACKNOWLEDGEMENTS

This work was mainly supported by a grant from the National Foundation for Sciences and Technology Development (NAFOSTED; 106.99-2010.76) in Viet Nam.

## REFERENCES

- Andersson H., Wetmore C., Lindqvist E., Luthman J., Olson L. 1997. Trimethyltin exposure in the rat induces delayed changes in brain-derived neurotrophic factor, fos and heat shock protein 70. *Neurotoxicology*. 18: 147-59.
- Calella AM, Nerlov C., Lopez RG., Sciarretta, C., von Bohlen und Halbach O., Bereshchenko O., Minichiello L. 2007. Neurotrophin/Trk receptor signaling mediates C/EBP $\alpha$ , - $\beta$  and NeuroD recruitment to immediate-early gene promoters in neuronal cells and requires C/EBPs to induce immediate-early gene transcription. *Neural. Dev.* DOI:10.1186/1749-8104-2-4.
- Cook LL., Stine KE., Reiter LW. 1984. Tin distribution in adult rat tissues after exposure to trimethyltin and triethyltin. *Toxicol. Appl. Pharmacol.* 76: 344-8.

- Huang, EJ., Reichardt, LF. 2003. Trk receptors: roles in neuronal signal transduction. 2003. *Annu. Rev. Biochem.* 72: 609–642.
- Kim HC., Bing G., Jhoo WK., Kim WK., *et al.*, 2002. Oxidative damage causes formation of lipofuscin-like substances in the hippocampus of the senescence-accelerated mouse after kainate treatment. *Behav. Brain. Res.* 131: 211–220.
- Minichiello L., Korte, M., Wolfner D., Kühn R., Unsicker K., Cestari V., *et al.*, 1999. Essential Role for TrkB Receptors in Hippocampus-Mediated Learning. *Neuron.* 24: 401-414.
- Moser VC., McGee JK., Ehman KD. 2009. Concentration and persistence of tin in rat brain and blood following dibutyltin exposure during development. *J. Toxicol. Environ. Health. A.* 72: 47-52.
- Noriko H., Shozo O., Takashi S., Satoshi M., Shoei F. 2010. Royal Jelly Facilitates Restoration of the Cognitive Ability in Trimethyltin-Intoxicated Mice. *J. Cell. Physiol.* 224: 710–721.
- Ogita K., Nishiyama N., Sugiyama C., Higuchi K., Yoneyama M., Yoneda Y. 2005. Regeneration of granule neurons after lesioning of hippocampal dentate gyrus: evaluation using adult mice treated with trimethyltin chloride as a model. *J. Neurosci. Res.* 82: 609–621.
- Segal RA. 2003. "Selectivity in Neurotrophin Signalling: Theme and Variations". *Annual Review of Neuroscience.* 26: 299–330.
- Tran HY., Shin EJ., Saito K., Nguyen XK., Chung, YH., *et al.*, 2012. Protective potential of IL-6 against trimethyltin-induced neurotoxicity in vivo. *Free. Radic. Biol. Med.* 52:1159-74.
- Yoneyama M., Nishiyama N., Shuto, M., Sugiyama, C., Kawada, K., *et al.*, 2008. In vivo depletion of endogenous glutathione facilitates trimethyltin-induced neuronal damage in the dentate gyrus of mice by enhancing oxidative stress. *Neurochem. Int.* 52: 761–769.